



VT-NMR and cytotoxic evaluation of some new *ortho*-(alkylchalcogen)acetanilides



Susana S. Ramos^{a,c}, Sandra S. Almeida^b, Paula M. Leite^b, Renato E.F. Boto^{b,c}, Samuel Silvestre^b, Paulo Almeida^{b,c,*}

^aUMTP-UBI, Unit of Textile and Paper Materials, University of Beira Interior, Rua Marquês d'Ávila e Bolama, 6201-001 Covilhã, Portugal

^bCICS-UBI—Health Sciences Research Centre, University of Beira Interior, Av. Infante D. Henrique, 6200-506 Covilhã, Portugal

^cDepartment of Chemistry, University of Beira Interior, Rua Marquês d'Ávila e Bolama, 6201-001 Covilhã, Portugal

ARTICLE INFO

Article history:

Received 27 June 2014

Received in revised form 15 September 2014

Accepted 17 September 2014

Available online 28 September 2014

Keywords:

Atropisomerism

Axial chirality

Cytotoxic evaluation

Dynamic VT-NMR

Nimesulide analogues

ortho-(Alkylchalcogen)acetanilides

ABSTRACT

Several novel atropisomeric *N*-alkyl-*N*-[(2-alkylchalcogen)phenyl]acetamides have been synthesized and fully characterized by ¹H and ¹³C NMR, FTIR, and HRMS (FAB). The barriers of the restricted rotation about the *N*-aryl bond between the two atropisomeric forms were measured by accurate lineshape simulation of variable temperature NMR (VT-NMR) spectra obtained in DMSO-*d*₆ solution and ranged from 17.0 to 20.5 kcal/mol. The relationship between the structure of the different acetanilide moieties and both coalescence temperature and energy of rotation are herein discussed. Taking in mind the acetamide structural resemblances with nimesulide related compounds known by their anticancer activity, the *in vitro* cytotoxicity of 20 representative acetanilides, against human breast (MCF-7) and prostate (LNCaP) cancer cell lines as well as normal human dermal fibroblasts (NHDF) was also preliminary evaluated. Interestingly a selective antiproliferative activity was observed for cancerous cells with prominence to LNCaP within the most potent *O*- and/or *N*-benzylic and -hexyl acetanilides.

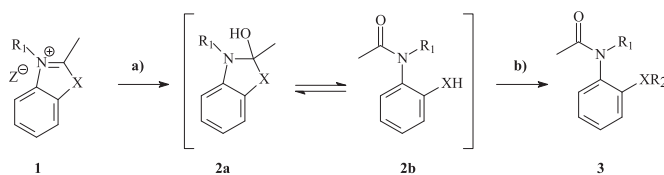
© 2014 Elsevier Ltd. All rights reserved.

1. Introduction

After the pioneering work by Curran et al. on atropisomeric anilides,¹ the potential use of non-biaryl atropisomers in medicinal chemistry has driven the interest and research around their synthesis and enantioselective synthesis, the stereoselectivity of their reactions as well as their use as chiral auxiliaries and chiral ligands.²

Recently, as part of our efforts to definitely clarify the identity of the products resulting from the hydroxylation of 2-methylbenzozolium iodides, we described the synthesis of some representative *ortho*-(alkylchalcogen)-*N*-ethylacetanilides **3** (X=O, S or Se, Scheme 1).³ The acetanilides **3** were obtained as atropisomers, in moderate to good yields, after an alkylation step used to trap the unstable sulfur and selenium open (as well as the more stable oxygen analogues) *N*-ethyl-(2-thiol/selenol/hydroxyl)acetanilide **2b**, resulting from the cleavage of the 2-hydroxybenzozole moiety of the initially formed intermediate **2a**.

N-Alkyl-(2-alkylchalcogen)acetanilides **3** have restricted rotations around their *N*-aryl bond as well as amide N–CO bond,



X = O, S, Se; Z = Br, I; R₁ and/or R₂ = Me, Et, Pr, Hex, Bn, 2-MeBn

Scheme 1. Reagents and conditions: (a) NEt₃, 96% ethanol, reflux; (b) ethanol, NaOH, RI or RBr, reflux.

affording, respectively, enantiomeric and diastereoisomeric forms.^{2q,3,4} This restricted rotation around the amide N–CO bond originates *endo* and *exo* isomers (benzene ring *cis* and *trans* to carbonyl oxygen), which are easily differentiated by ¹H NMR. In general, *N*-substituted anilides exist predominantly as the *exo* isomer.^{2q,3–5} The atropisomeric forms resulting from the circumscribed rotation about the amide *N*-aryl bond are easily recognized in solution by the signals of the two magnetically nonequivalent geminal *N*-CH₂ protons clearly displayed in the ¹H NMR spectra. The dynamic process of the *E* diastereoisomer of five representative acetanilides **3** was thus investigated by variable temperature NMR (VT-NMR) spectroscopy and the corresponding rotation barriers

* Corresponding author. Tel.: +351 275329174; fax: +351 275319056; e-mail addresses: paulo.almeida@ubi.pt, pjsa@ubi.pt (P. Almeida).

(ΔG^\ddagger) at 298 K and the coalescence temperatures (T_c) were determined, ever since is less than 413 K.³

Following our preliminary results,³ herein we describe a full set of 23 *ortho*-substituted acetanilides **3a–h** (X=O), **3i–u** (X=S), and **3v,w** (X=Se), 18 of them are, to the best of our knowledge, novel (**3b, d–h, j, l–u, w**). In this serial, the nature of the chalcogen atom (X) and the nature of the alkyl group linked to both amide group (R_1) or chalcogen atom (R_2) were varied (Scheme 1, Table 1).

Hence, the full characterization by ¹H and ¹³C NMR, FTIR, and HRMS (FAB) of these atropisomeric *N*-alkyl-*N*-[(2-alkylchalcogen)phenyl]acetamides **3a–j, l–w** are here presented. The ΔG^\ddagger between the two atropisomeric forms of acetanilides **3a–w**, with emphasis for alkoxy- **3a–h** and alkylthioanilides **3i–u**, have been determined by accurate lineshape simulation of VT-NMR spectra obtained in DMSO-*d*₆ solution and ranged from 17.0 to 20.5 kcal/mol. The relationship between the structure of the different moieties of acetanilides and both T_c and ΔG^\ddagger for all acetanilides is herein discussed. The cytotoxicity against normal human dermal fibroblasts (NHDF) and human breast (MCF-7) and prostate (LNCaP) cancer cell lines of several representative acetanilides **3a–d, g–m, q–w** and anilines **4a, b** additionally prepared was also evaluated and is here also presented and discussed.

Table 1

Reaction times, overall yields, ΔG^\ddagger and T_c for *N*-alkyl-(2-alkylchalcogen)acetanilides **3**

Compd 3	X	R_1	R_2	Reaction times		Yield ^a (%)	ΔG^\ddagger (± 0.2 kcal/mol)	T_c (K)
				Step (a) (min)	Step (b) (h)			
a ^b	O	Et	Et	60	3	79	18.1	388
b	O	Et	Pr	45	4	70	17.9	391
c ^b	O	Et	Hex	60	6	68	17.1	393
d	O	Et	Bn	45	6	66	17.2	393
e	O	Pr	Et	45	3	71	18.1	395
f	O	Pr	Hex	45	6	65	17.9	398
g	O	Hex	Pr	60	5	71	17.4	401
h	O	Bn	Et	60	3	64	17.0	402
i ^b	S	Et	Et	30	3	87	18.3	c
j	S	Et	Pr	30	4	77	18.2	c
k ^b	S	Et	Hex	30	6	75	17.8	c
l	S	Et	Bn	30	6	78	18.0	c
m	S	Pr	Me	30	3	82	18.1	c
n	S	Pr	Et	30	3	81	18.2	c
o	S	Pr	Hex	30	6	69	18.1	c
q	S	Hex	Et	45	3	84	18.0	c
p	S	Hex	Pr	45	6	72	17.5	c
r	S	Bn	Et	30	3	83	17.5	c
s	S	Bn	Bn	45	5	65	17.9	c
t	S	MeBn	Et	45	5	62	18.1	c
u	S	MeBn	MeBn	60	6	59	18.2	c
v ^b	Se	Et	Et	30	4	85	20.5	c
w	Se	Et	Hex	45	5	74	17.8	c

^a Isolated overall yield.

^b Previously described.³

^c >413 K.

2. Results and discussion

In our previous described work,³ the nature of both alkyl groups were restricted to *N*-ethylacetanilides (**3**, R_1 =Et) and to *ortho*-(ethylchalcogen)- and *ortho*-(hexylchalcogen)acetanilides (**3**, X=O, S, Se; R_2 =Et, Hex).

Thus, in order to determine a more accurate relationship between the structure of the different moieties of acetanilides and both T_c and ΔG^\ddagger , a set of 18 new acetanilides was synthesized in addition to the 5 previously described. In this series, the nature of the chalcogen atom as well as the *N*-acetamide and chalcogen substituents were varied [X=O, S or Se; R_1 and/or R_2 =methyl, ethyl, propyl, hexyl, benzyl (Bn), and/or 2-methylbenzyl (MeBn) (Scheme 1)].

All *N*-alkyl-(2-alkylchalcogen)acetanilides **3** were prepared from the appropriate 3-alkyl-2-methylbenzazol-3-ium iodides **1** (or bromides), in moderate to good yields, following the same procedure already described³ (Scheme 1, Table 1). In our hands, none *O*-alkylated products of **2a** were observed, which is in agreement with the more expectable nucleophilic anionic forms of thiophenol, selenophenol, and phenol moieties present in acetanilides **2b** in relation to the alkoxy form present in **2a**.

All the new acetanilides **3** were structurally characterized by ¹H and ¹³C NMR, FTIR, and HRMS (FAB).

As expected, the ¹H NMR analysis reveals four stereoisomeric forms, as already stressed in our previous work.³ The R_a and S_a *exo* forms were always predominant with an *E/Z* ratio $\geq 95:5$, as usual for *N*-substituted anilides.^{3–5} As example, both axially enantiomeric forms S_a -*endo* and S_a -*exo*, are present in Fig. 1.

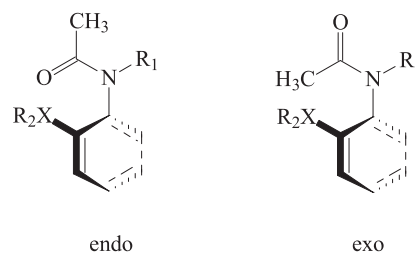


Fig. 1. S_a -*endo* and S_a -*exo* axially enantiomeric forms of acetanilides **3**.

Since the *exo* diastereoisomer is almost the exclusive form, the ΔG^\ddagger between the two axially enantiomeric forms (S_a and R_a) in solution have been determined by accurate lineshape simulation of VT-NMR spectra using gNMR modeling software (Cherwell Scientific). These lineshape simulations were based on the experimental spectra obtained for each compound, namely on the chemical shifts and coupling constants of both two geminal *N*-CH₂ protons magnetically nonequivalent and on the distance between both signals. ¹H NMR representative pattern signals of one of the *N*-CH₂ geminal proton of acetanilides are presented in Fig. 2.

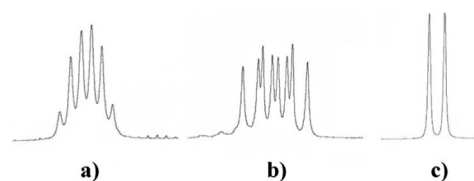


Fig. 2. ¹H NMR representative pattern signals (400 MHz; DMSO-*d*₆) of one of the geminal *N*-CH₂ proton: (a) R_1 =Et; (b) R_1 =Pr or Hex; and (c) R_1 =Bn.

Lineshape simulation of the spectra using gNMR modeling software gave a rate constant for interconversion (k) at a range of temperatures (T in K), which was converted into a barrier to rotation at a given temperature using the Eyring equation.⁶

$$\Delta G^\ddagger = 4.569 \times 10^{-3} T (10.319 + \log T/k)$$

As a representative example, both experimental and simulated ¹H NMR *N*-CH₂ signals of the *N*-ethyl-*N*-(2-propoxyphenyl)acetamide **3b**, from 298 to 391 K (k variation from 1 to 225 s⁻¹) are presented in Fig. 3.

The Eyring plot of $\ln(k/T)$ versus $1/T$ gives a straight line from which, using the equation $y=mx+c$, the slope (m) gives the enthalpy of rotation (ΔH^\ddagger) and the y -intercept (c) gives the entropy of rotation (ΔS^\ddagger) as described above. Inserting these values into Gibbs' equation for free energy ($\Delta G^\ddagger = \Delta H^\ddagger - T\Delta S^\ddagger$) gives an estimation of the

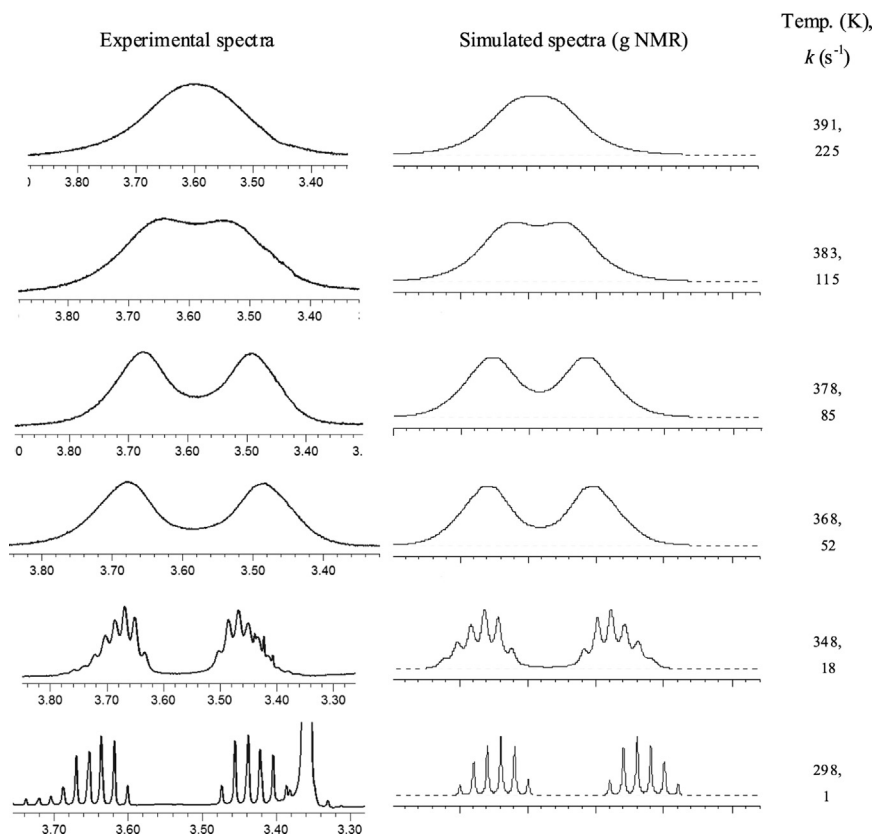


Fig. 3. Experimental (left) ^1H NMR spectra of $N\text{-CH}_2$ protons of **3b** in $\text{DMSO-}d_6$ as a function of temperature and lineshape simulation (right) for the same compound using gNMR software with the rate constants for the interconversion between the two rotamers.

ΔG^\ddagger at room temperature (taken to be 25°C). Eyring plots $\ln(k/T)$ versus $1/T$ for alkyloxyacetanilide **3b** and alkylthioacetanilide **3j** were also present as representative examples (Fig. 4) as well as the activation parameters determined from these plots (Table 2).

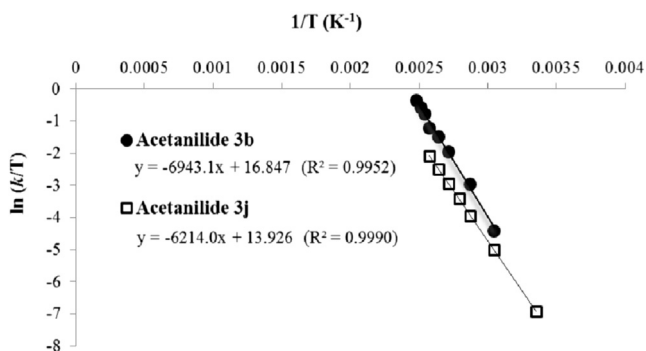


Fig. 4. Representative Eyring plots of $\ln(k/T)$ versus $1/T$ for acetanilides **3b** and **3j**.

Table 2
Representative acetanilides **3b** and **3j** activation parameters determined from plots of $\ln(k/T)$ versus $1/T$ using Eyring equation

	m	ΔH^\ddagger (J)	c	ΔS^\ddagger (J)	ΔG^\ddagger (J)
3b	-6943.1	57,728.2	16.847	-57.5	74,871.8
3j	-6214.0	51,666.1	13.926	-81.8	76,054.8

In our case, the linear regression analysis performed for each compound **3a–w** was obtained from a set of 7 to 12 data points, with correlation coefficients between 0.9873 and 0.9990, showing consistently a very high degree of linearity for the data obtained.

However, T_c was not achieved for *ortho*-(alkylthio)- **3i–u** and *ortho*-(alkylseleno)acetanilides **3v,w** and therefore rate constants determined above this temperature could not be measured. The estimated ΔG^\ddagger ranging from 17.0 to 20.5 kcal/mol (Table 1, compounds **3a–w**) are in accordance with the values disclosed in the literature for anilides possessing a single bulky *ortho*-substituent.^{1,2p,q,7} The T_c from 388 to 402 K herein presented are restricted for the *ortho*-(alkyloxy)acetanilides **3a–h**, ever since the lowest temperatures at which the two rotamers of remaining acetanilides **3i–w** merge were determined to be above the maximum spectrometer's working temperature (413 K).

Despite the fact that acetanilides **3** show the same $N\text{-CH}_2$ geminal protons splitting patterns within the same alkyl group linked to the chalcogen atom serial (Fig. 2), they differ in the region where these signals are displayed [δ 3.33–5.01 ppm ($X=\text{O}$); δ 2.97–5.42 ppm ($X=\text{S}$); δ 3.08–3.95 ppm ($X=\text{Se}$)]. Another significant difference lies on the chemical shift difference ($\Delta\delta_{\text{AB}}$) between the two geminal $N\text{-CH}_2$ protons, with the values being higher as the size of the chalcogen atom increases from oxygen to sulfur [$\Delta\delta_{\text{AB}}$ from 0.21 to 0.55 ($X=\text{O}$); $\Delta\delta_{\text{AB}}$ from 0.82 to 1.51 ($X=\text{S}$)]. This observation is in agreement with the $\Delta\delta_{\text{AB}}$ between nonequivalent methylene protons observed for other acetanilides already described, where $\Delta\delta_{\text{AB}}$ also depends on the size of the *ortho*-substituent of the aniline moiety.^{4a,d} However, when the size of the chalcogen increases from sulfur to selenium atom, the shift differences remain almost the same within the two alkylselenoacetanilides **3v,w** compared to their thio-congeners **3i,k**.

Another direct consequence of the size of the chalcogen is the T_c of the acetanilides. As a matter of this fact, while the T_c of *ortho*-(alkyloxy)acetanilides **3a–h** was determined to be below 413 K, for *ortho*-(alkylthio) **3i–u** and (alkylseleno)acetanilides **3v,w** we are not able to reach the coalescence due to the limitation of the

spectrometer's working temperature, as above mentioned. In addition, within the set of *ortho*-(alkyloxy)acetanilides **3a–h**, the T_c raises with the increase of the size of both R_1 and R_2 *n*-alkyl groups (Hex>Prop>Et).

The previously described relationship between the rotation barrier values with both alkyl R_1 and R_2 size groups based just on five different acetanilides,³ are herein reconfirmed. Specifically, ΔG^\ddagger values slightly increase with the size of the chalcogen (Se>S>O). Nevertheless, and in contrary to our expectations, the increase in the rotational barrier in function of the alkyl group size (Hex>Prop>Et) within each chalcogen serial renders lower ΔG^\ddagger values, in accordance with our previous report.³ This statement is reinforced by the lower ΔG^\ddagger value observed when the hexyl or benzylic (benzyl and 2-methylbenzyl) group is introduced in R_1 or R_2 position.

Taking into account the structural similarity between the acetanilides herein described and nimesulide related compounds as anticancer agents,⁸ we decided to evaluate the in vitro antiproliferative effect against normal human dermal fibroblasts (NHDF) and against the human hormone-dependent breast (MCF-7), and prostate (LNCaP) cancer cell lines, for several representative *ortho*-(alkyloxy)acetanilides **3a–d,g,h**, *ortho*-(alkylthio)acetanilides **3i–m,q–u**, and *ortho*-(alkylseleno)acetanilides **3v,w**. In order to evaluate the carbonyl group role in the cytotoxicity of these acetanilides, two representative *ortho*-(alkylchalcogen)-*N,N*-dialkylanilines **4a,b** were additionally prepared as previously described³ and their in vitro antiproliferative activity evaluated and compared to their *ortho*-(alkylthio)acetanilides **3i,m** congeners.

The evaluation of the relative cell viability of MCF-7, NHDF, and LNCaP cells was performed through the MTT assay, following a previously described procedure.⁹ Briefly, cells were seeded in 48-well plates and treated with a 30 μ M concentration of the different compounds during approximately 48 h, with untreated cells serving as negative control and H_2O_2 (1 mM) as positive control and at the end of incubation the MTT test was effected. The results of these experiments are presented in Table 3.

Table 3
Relative cell viability of MCF-7, NHDF, and LNCaP cells incubated with compounds **3a–d,g–m,q–w** and **4a,b** at 30 μ M, determined by the MTT assay after 48 h of exposition. Mean values \pm SD (% of the negative control) were obtained from five experimental determinations and data are expressed as a percentage of cell viability in comparison with the respective negative control

Entry	Compound (30 μ M)	MCF-7	LNCaP	NHDF	log P^a
1	3a	93.45 \pm 3.38	68.32 \pm 10.63	85.59 \pm 10.74	1.73
2	3b	92.54 \pm 3.64	74.29 \pm 10.14	83.97 \pm 6.84	2.21
3	3c	55.53 \pm 4.85	38.46 \pm 2.62	78.34 \pm 7.75	3.47
4	3d	88.84 \pm 2.70	52.97 \pm 4.41	75.77 \pm 2.96	3.12
5	3g	51.52 \pm 9.41	45.86 \pm 2.01	84.34 \pm 5.20	3.95
6	3h	87.59 \pm 3.58	65.75 \pm 10.13	91.07 \pm 12.63	3.12
7	3i	99.50 \pm 5.98	75.99 \pm 9.89	82.65 \pm 3.13	2.29
8	3j	89.14 \pm 7.94	59.74 \pm 4.03	76.19 \pm 6.36	2.78
9	3k	67.65 \pm 5.63	53.19 \pm 6.17	83.48 \pm 8.95	4.03
10	3l	95.33 \pm 7.97	51.71 \pm 5.02	79.17 \pm 7.78	3.69
11	3m	95.34 \pm 6.77	65.78 \pm 2.66	81.49 \pm 4.77	1.96
12	3q	47.58 \pm 6.46	59.65 \pm 9.99	82.99 \pm 8.86	4.52
13	3r	89.37 \pm 5.62	62.44 \pm 3.19	80.05 \pm 6.03	3.69
14	3s	79.81 \pm 5.21	52.63 \pm 6.08	96.68 \pm 12.68	5.08
15	3t	77.00 \pm 7.68	41.85 \pm 1.75	75.21 \pm 6.90	4.18
16	3u	13.71 \pm 4.71	39.03 \pm 2.59	79.02 \pm 10.39	6.06
17	3v	98.23 \pm 5.71	86.20 \pm 8.98	95.45 \pm 8.18	1.88
18	3w	82.63 \pm 6.97	59.35 \pm 1.60	98.90 \pm 7.91	3.47
19	4a	99.72 \pm 3.40	83.65 \pm 6.86	93.00 \pm 6.44	3.77
20	4b	97.19 \pm 2.32	76.91 \pm 16.91	88.27 \pm 7.15	3.43
21	H_2O_2 (1 mM)	0.17 \pm 0.32	11.22 \pm 1.67	1.51 \pm 2.56	—

^a Calculated lipophilicity, using the software ChemDraw 9.0 (CambridgeSoft).

Considering the data presented in Table 3 it is clear that, despite a low to moderate antiproliferative activity, generally these compounds seems to be more toxic to LNCaP cells than to MCF-7 and NHDF cells. Moreover, the benzylic **3d,h,i,r–u** and hexyl **3c,g,k,q,w**

acetanilides (Table 2, entries 3–6, 9, 10, 12–16, 18) revealed to be more toxic and more selective (frequently up to 2-fold) to both cancer cell lines than the corresponding methyl, ethyl, and propyl congeners.

These results prompt us to suspect that the lipophilicity of the compounds could be related to their antiproliferative activity. Thus, by using the software ChemDraw 9.0, the log P of all compounds considered in this assay was calculated (Table 3) and the relationship between these two variables was evaluated. From this analysis, only a modest association between the lipophilicity and cytotoxic effects was found for LNCaP cells ($r^2=0.5379$) and for MCF-7 cells ($r^2=0.3933$) and no association was evidenced for NHDF cells ($r^2=0.0032$). Moreover, a careful analysis within X_2N_2 , X_6N_2 , and X_3N_6 series [Table 3, entries 1, 3, 5, 7, 9, 12, 17, and 18; X_n and N_n mean the number of carbons (2=ethyl, 3=propyl, and 6=hexyl) linked to the chalcogen (X=O, S or Se) or nitrogen, respectively] reveals a generally higher cytotoxicity for the *ortho*-(alkyloxy)acetanilides (X=O) and a lower one for the *ortho*-(alkylseleno)acetanilides (X=Se).

The *ortho*-(alkylthio)anilines **4a,b** (Table 3, entries 19 and 20) revealed to be less active and less selective than their *ortho*-(alkylthio)acetanilides **3i,m** congeners (Table 3, entries 7 and 11), pointing to the importance of the carbonyl amide group for the antiproliferative activity and to their needless reduction into a methylene group.

The highest antiproliferative activity and superior selectivity against both cancerous cells (almost 6-fold and 2-fold higher for MCF-7 and LNCaP, respectively, when compared to NHDF cells) observed for the 2-methylbenzyl disubstituted thioacetanilide **3u** (Table 3, entry 16) should be emphasized. In fact, this compound revealed to have a higher selectivity to breast cancer cells (13.71% proliferation vs control) in comparison to both prostate (39.03%) and normal skin fibroblasts (79.02%). This important result is now being explored in order to clarify the potential interest of this compound as a future antitumor agent. Moreover, when comparing acetanilides **3u** and **3s** (Table 3, entries 16 and 14) it is clear that the introduction of an *ortho*-methyl group increases the antiproliferative activity of the benzylic moiety as well as in their selectivity for MCF-7 cells in special. A similar effect can also be observed for compounds **3t** and **3r**, and again the *ortho*-methylated (**3t**) revealed a higher antiproliferative effect than the non-methylated derivative (**3r**) (Table 3, entries 15 and 13).

As the highest antiproliferative effects in cancer cell lines were observed with compound **3u**, we also performed dose–response studies with this and with compound **3q**, aiming to obtain their half-medium inhibitory concentration (IC₅₀) values. For this, cells were treated with six different concentrations (0.01, 0.1, 1, 10, 50, and 100 μ M) of the compounds, again during nearly 48 h, before the MTT test and the dose–response curves and IC₅₀ values were established by sigmoid fitting. This study not only confirmed the relevant cytotoxic effects of these compounds in these cells but also revealed that the anilide **3u** has an interesting IC₅₀ value in LNCaP cells. In fact, considering a 95% confidence interval, the IC₅₀ values for compounds **3u** and **3q** in LNCaP cells were 17.24 μ M ($r^2=0.8632$) and 61.64 μ M ($r^2=0.8723$), and in MCF-7 cells were 40.93 μ M ($r^2=0.9422$; 95% CI) and 41.84 μ M ($r^2=0.9407$), respectively. As these compounds presented relatively low cytotoxicity against NHDF cells we decided not to determine the IC₅₀ values with these non-cancerous cells.

Although more studies are needed to further explore the potential interest of this acetanilide family as antiproliferative agents, particularly those based in hexyl or substituted benzylic (as acetanilide **3u**) groups, the results herein presented, can be significantly important for the future development of more selective and powerful structures.

3. Conclusions

In summary, we prepared a series of atropisomeric *ortho*-(alkylchalcogen)-*N*-alkylacetanilides **3** from quaternary ammonium salts **1** in overall yields of 59–87%.

The dynamics of the *N*-aryl bond rotation of the major *E* diastereoisomers of these acetanilides have been evaluated by VT-NMR techniques and computed by gNMR calculations. While the magnitude of the energetic barrier to the interconversion between atropisomers is just slightly dependent on the chalcogen and on the nature of both alkyl groups linked to *N*-aryl or to the chalcogen atom, the T_c appears to be much more structurally dependent.

The evaluation of the in vitro antiproliferative effects of a range of representative acetanilides against normal human dermal fibroblasts (NHDF) and MCF-7 and LNCaP cancer cell lines was also performed. Curiously, this study revealed not only a general selective cytotoxicity against tumor cells versus normal cells, especially pronounced for prostate cancer cells, but also that benzylic and hexyl acetanilides were the most powerful compounds. The best result was observed for the methylphenyl disubstituted acetanilide (compound **3v**), which is now being studied as a potential future lead compound as anti-breast cancer agent. In order to enlarge structure–activity relationship data in this context, the development of new hexylic and/or benzylic related acetanilides is also now object of our interest.

Additionally, this new synthetic way to prepare *ortho*-(alkylchalcogen)-*N*-alkylacetanilides **3** appears to be a promising alternative to develop new compounds resembling nimesulide, especially in cases where the benzothiazole starting material possesses a nitro group or other electrowithdrawing group derived from in the 6-position. Besides, other steps as acetanilide hydrolyze followed by aniline derivatization could be considered.

Finally, it is our belief that our search for more interesting related compounds will forward us to acetanilides with a second bulky *ortho*-substituted group and therefore presenting a ΔG^\ddagger sufficiently high to allow isolation of stereochemically stable atropisomers by this new simple, effective, and regiospecific way herein depicted. Thus, an energy of rotation high enough to allow the separation and isolation of both atropisomers of each acetanilide will open to us the opportunity to study their biological interest, such as the cytotoxicity against various human cancer cell lines, both as racemic or as their isolated atropisomeric forms.

4. Experimental

4.1. General considerations

Reagents and solvents were purchased from standard sources and purified and/or dried whenever necessary using standard procedures prior to use. TLC analysis was performed routinely using 0.20 mm Al-backed silica-gel plates (Macherey–Nagel 60 F₂₅₄). Compounds were visualized using UV light (254 nm). Attenuated total reflectance (ATR) IR spectra were collected on a Thermo-scientific Nicolet iS10: smart ITR, equipped with a diamond ATR crystal. For ATR data acquisition, a drop of the sample oil was placed onto the crystal and the spectrum was recorded. An air spectrum was used as a reference in absorbance calculations. The sample spectra were collected at room temperature in the 4000–400 cm⁻¹ range by averaging 32 scans at a spectral resolution of 2 cm⁻¹. NMR spectra were acquired on a Bruker Avance 400 MHz spectrometer (¹H NMR at 400 MHz and ¹³C NMR at 100 MHz) and were processed with the software TOPSPIN 3.1 (Bruker, Fitchburg, WI, USA). Deuterated dimethylsulfoxide (DMSO-*d*₆) was used as solvent. Chemical shifts are reported in parts per million (δ) relative to TMS or deuterated solvent as an

internal standard. Coupling constants (*J* values) are reported in hertz (Hz) and splitting multiplicities are described as s=singlet; d=doublet; t=triplet; q=quartet; or combinations of the above; or m=multiplet. All new compounds were determined to be >95% pure by ¹H NMR. ESI-TOF mass spectrometry was performed on a microTOF (focus) mass spectrometer (Bruker Daltonics, Bremen, Germany). Ions were generated using an Apollo II (ESI) source. Ionization was achieved by electrospray, using a voltage of 4500 V applied to the needle, and a counter voltage between 100 and 150 V applied to the capillary. Samples were prepared by adding a spray solution of 70:30 (v/v) acetonitrile/water with 0.1% of formic acid into a solution of the sample in CH₂Cl₂ at a v/v ratio of 1 to 5% to give the best signal-to-noise ratio. Data acquisition was performed using the microTOFControl software version 2.1, and data processing was performed using the DataAnalysis software, version 3.4 both from Bruker Daltonics.

4.2. Synthesis and structural characterization

The acetanilides **3a–w** and anilines **4a,b** were prepared as already described.³ The characterization of both novel or not yet fully characterized acetanilides **3a–g,k–w** and aniline **4a** described herein is presented.

4.2.1. *N*-(2-Ethoxyphenyl)-*N*-ethylacetamide **3a.** IR ($\nu_{\max}/\text{cm}^{-1}$): 2980, 2931, 1682, 1651 (C=O), 1596, 1500, 1455, 1403, 1264, 1231, 1043, 924, 732, 702. ¹H NMR (400 MHz, DMSO-*d*₆): δ =7.34 (dt, 1H, *J*=6.0, 1.7 Hz), 7.22 (dd, 1H, *J*=7.5, 1.7 Hz), 7.13 (dd, 1H, *J*=7.2, 1.1 Hz), 6.99 (dt, 1H, *J*=6.2, 1.3 Hz), 4.02–4.15 (m, 2H), 3.65 (dq, 1H, *J*=13.7, 7.0 Hz), 3.43 (dq, 1H, *J*=13.7, 7.0 Hz), 1.64 (s, 3H), 1.30 (t, 3H, *J*=7.0 Hz), 0.96 (t, 3H, *J*=7.0 Hz) ppm. ¹³C NMR (100 MHz, DMSO-*d*₆): δ =169.6, 154.7, 131.4, 130.3, 129.8, 121.3, 113.7, 64.0, 42.6, 22.4, 15.1, 13.3 ppm. HRMS (ESI-TOF) *m/z* 208.13391 (208.13375 calcd for C₁₂H₁₈NO₂, [M+H⁺]).

4.2.2. *N*-Ethyl-*N*-(2-propoxyphenyl)acetamide **3b.** IR ($\nu_{\max}/\text{cm}^{-1}$): 2968, 2934, 2877, 1655 (C=O), 1596, 1499, 1454, 1395, 1286, 1265, 1231, 1043, 978, 750. ¹H NMR (400 MHz, DMSO-*d*₆): δ =7.34 (dt, 1H, *J*=7.8, 1.7 Hz), 7.22 (dd, 1H, *J*=7.6, 1.7 Hz), 7.13 (dd, 1H, *J*=8.3, 1.0 Hz), 6.99 (dt, 1H, *J*=7.5, 1.2 Hz), 3.98 (t, 2H, *J*=5.9 Hz), 3.65 (dq, 1H, *J*=13.9, 7.0 Hz), 3.43 (dq, 1H, *J*=13.9, 7.0 Hz), 1.70 (sext, *J*=6.9, 2H), 1.63 (s, 3H), 0.96 (dt, 3H, *J*=7.4, 1.6 Hz) ppm. ¹³C NMR (100 MHz, DMSO-*d*₆): δ =169.7, 155.0, 131.4, 130.2, 129.8, 121.3, 113.6, 69.7, 42.8, 22.7, 22.4, 13.4, 11.0 ppm. HRMS (ESI-TOF) *m/z* 222.14940 (222.14940 calcd for C₁₃H₂₀NO₂, [M+H⁺]).

4.2.3. *N*-Ethyl-*N*-[2-(hexyloxy)phenyl]acetamide **3c.** IR ($\nu_{\max}/\text{cm}^{-1}$): 2960, 2931, 2871, 1657 (C=O), 1595, 1499, 1455, 1397, 1283, 1264, 1231, 1013, 935, 750. ¹H NMR (400 MHz, DMSO-*d*₆): δ =7.34 (dt, 1H, *J*=7.8, 1.8 Hz), 7.21 (dd, 1H, *J*=7.8, 1.8 Hz), 7.13 (dd, 1H, *J*=8.3, 1.0 Hz), 6.99 (dt, 1H, *J*=7.6, 1.3 Hz), 4.00 (t, 2H, *J*=6.3 Hz), 3.64 (dq, 1H, *J*=13.8, 6.9 Hz), 3.43 (dq, 1H, *J*=13.8, 6.9 Hz), 1.64–1.72 (m, 2H), 1.62 (s, 3H), 1.36–1.43 (m, 2H), 1.26–1.32 (m, 4H), 0.95 (t, 3H, *J*=7.1 Hz), 0.86 (t, 3H, *J*=7.1 Hz) ppm. ¹³C NMR (100 MHz, DMSO-*d*₆): δ =169.5, 154.9, 131.3, 130.2, 129.8, 121.2, 113.5, 68.0, 42.6, 31.3, 29.0, 25.5, 22.5, 22.2, 14.3, 13.3 ppm. HRMS (ESI-TOF) *m/z* 264.19524 (264.19635 calcd for C₁₆H₂₆NO₂, [M+H⁺]).

4.2.4. *N*-[2-(Benzyloxy)phenyl]-*N*-ethylacetamide **3d.** IR ($\nu_{\max}/\text{cm}^{-1}$): 2972, 2932, 2872, 1652 (C=O), 1595, 1499, 1401, 1397, 1282, 1264, 1222, 1075, 950, 750, 735. ¹H NMR (400 MHz, DMSO-*d*₆): δ =7.41–7.44 (m, 3H), 7.35–7.40 (m, 2H), 7.30–7.34 (m, 1H), 7.24–7.27 (m, 2H), 7.03 (dt, 1H, *J*=7.5, 1.5 Hz), 5.14–5.21 (m, 2H), 3.72 (dq, 1H, *J*=13.4, 7.0 Hz), 3.41 (dq, 1H, *J*=13.4, 7.0 Hz), 1.65 (s, 3H), 0.96 (t, 3H, *J*=7.2 Hz) ppm. ¹³C NMR (100 MHz, DMSO-*d*₆): δ =169.7, 154.6, 137.4, 131.6, 130.5, 129.9, 129.0, 129.0, 128.4, 127.8,

127.8, 121.7, 114.2, 70.0, 42.7, 22.4, 13.4 ppm. HRMS (ESI-TOF) m/z 270.14819 (270.14940 calcd for $C_{17}H_{20}NO_2$, $[M+H^+]$).

4.2.5. *N*-(2-Ethoxyphenyl)-*N*-propylacetamide **3e.** IR ($\nu_{\max}/\text{cm}^{-1}$): 2966, 2933, 2875, 1652 (C=O), 1596, 1499, 1455, 1398, 1281, 1249, 1221, 1122, 1043, 923, 751, 734. ^1H NMR (400 MHz, DMSO- d_6): δ =7.34 (dt, 1H, J =7.8, 1.6 Hz), 7.22 (dd, 1H, J =7.8, 1.6 Hz), 7.13 (dd, 1H, J =8.0, 1.2 Hz), 6.99 (dt, 1H, J =7.6, 1.2 Hz), 4.05–4.13 (m, 2H), 3.58 (ddd, 1H, J =13.2, 8.8, 6.7 Hz), 3.55 (ddd, 1H, J =13.2, 8.6, 6.8 Hz), 1.64 (s, 3H), 1.34–1.42 (m, 2H), 1.30 (t, 3H, J =7.1 Hz), 0.81 (t, 3H, J =7.6 Hz) ppm. ^{13}C NMR (100 MHz, DMSO- d_6): δ =169.9, 154.7, 131.6, 130.2, 129.7, 121.2, 113.6, 64.2, 49.6, 22.2, 21.1, 15.1, 11.8 ppm. HRMS (ESI-TOF) m/z 222.14959 (222.14940 calcd for $C_{13}H_{20}NO_2$, $[M+H^+]$).

4.2.6. *N*-[2-(Hexyloxy)phenyl]-*N*-propylacetamide **3f.** IR ($\nu_{\max}/\text{cm}^{-1}$): 2956, 2930, 2872, 1657 (C=O), 1595, 1499, 1455, 1395, 1280, 1248, 1221, 1123, 1044, 1014, 937, 750. ^1H NMR (400 MHz, DMSO- d_6): δ =7.33 (dt, 1H, J =7.8, 1.8 Hz), 7.21 (dd, 1H, J =7.6, 1.8 Hz), 7.12 (dd, 1H, J =8.3, 1.2 Hz), 6.98 (dt, 1H, J =7.5, 1.2 Hz), 4.00 (t, 2H, J =6.1 Hz), 3.58 (ddd, 1H, J =13.2, 8.4, 6.4 Hz), 3.33 (ddd, 1H, J =13.2, 8.8, 6.1 Hz), 1.64–1.72 (m, 2H), 1.63 (s, 3H), 1.33–1.43 (m, 4H), 1.26–1.31 (m, 4H), 0.86 (t, 3H, J =6.8 Hz), 0.80 (t, 3H, J =7.5 Hz) ppm. ^{13}C NMR (100 MHz, DMSO- d_6): δ =169.9, 154.9, 131.7, 130.1, 129.8, 121.2, 113.5, 68.0, 49.5, 31.2, 29.0, 25.5, 22.5, 22.2, 21.1, 14.3, 11.7 ppm. HRMS (ESI-TOF) m/z 278.21234 (278.21200 calcd for $C_{17}H_{28}NO_2$, $[M+H^+]$).

4.2.7. *N*-Hexyl-*N*-(2-propoxyphenyl)acetamide **3g.** IR ($\nu_{\max}/\text{cm}^{-1}$): 2958, 2928, 2872, 2858, 1656 (C=O), 1596, 1499, 1454, 1395, 1274, 1257, 1235, 1122, 1044, 978, 750, 727. ^1H NMR (400 MHz, DMSO- d_6): δ =7.33 (dt, 1H, J =7.9, 1.8 Hz), 7.21 (dd, 1H, J =7.6, 1.8 Hz), 7.12 (dd, 1H, J =8.2, 1.0 Hz), 6.99 (dt, 1H, J =7.5, 1.0 Hz), 3.97 (t, 2H, J =6.2 Hz), 3.60 (ddd, 1H, J =13.2, 8.0, 6.7 Hz), 3.39 (ddd, 1H, J =13.2, 8.0, 6.6 Hz), 1.70 (sext, 2H, J =7.0 Hz), 1.63 (s, 3H), 1.29–1.39 (m, 2H), 1.15–1.25 (m, 6H), 0.96 (t, 3H, J =7.6 Hz), 0.82 (t, 3H, J =7.0 Hz) ppm. ^{13}C NMR (100 MHz, DMSO- d_6): δ =169.8, 154.8, 131.6, 130.0, 129.7, 121.2, 113.5, 69.6, 47.8, 31.6, 27.8, 26.5, 22.5, 22.5, 22.2, 14.3, 10.9 ppm. HRMS (ESI-TOF) m/z 278.21166 (278.21200 calcd for $C_{17}H_{28}NO_2$, $[M+H^+]$).

4.2.8. *N*-benzyl-*N*-(2-ethoxyphenyl)acetamide **3h.** IR ($\nu_{\max}/\text{cm}^{-1}$): 2984, 2930, 1738, 1652 (C=O), 1500, 1396, 1264, 1217, 1044, 733, 701. ^1H NMR (400 MHz, DMSO- d_6): δ =7.20–7.35 (m, 4H), 7.17 (d, 2H, J =7.4 Hz), 7.07 (d, 1H, J =8.0 Hz), 7.02 (dd, 1H, J =8.0, 1.4 Hz), 6.88 (t, 1H, J =7.6 Hz), 5.01 (d, 1H, J =15.7 Hz), 4.46 (d, 1H, J =14.9 Hz), 3.88–4.10 (m, 2H), 1.74 (s, 3H), 1.27 (t, 3H, J =7.4 Hz) ppm. ^{13}C NMR (100 MHz, DMSO- d_6): δ =170.5, 154.4, 138.2, 131.3, 130.0, 129.8, 128.6, 128.6, 128.5, 128.5, 127.4, 121.0, 113.7, 64.0, 51.4, 22.2, 15.0 ppm. HRMS (ESI-TOF) m/z 270.14944 (270.14940 calcd for $C_{17}H_{20}NO_2$, $[M+H^+]$).

4.2.9. *N*-Ethyl-*N*-[2-(ethylthio)phenyl]acetamide **3i.** IR ($\nu_{\max}/\text{cm}^{-1}$): 2972, 2930, 2872, 1655 (C=O), 1582, 1567, 1470, 1441, 1392, 1296, 1263, 1245, 1144, 1102, 1080, 1063, 1035, 994, 918, 759, 734. ^1H NMR (400 MHz, DMSO- d_6): δ =7.38–7.40 (m, 2H), 7.21–7.23 (m, 2H), 3.94 (dq, 1H, J =14.0, 7.1 Hz), 3.08 (dq, 1H, J =14.0, 7.1 Hz), 2.98 (q, 2H, J =7.0 Hz), 1.62 (s, 3H), 1.25 (t, 3H, J =6.9 Hz), 0.99 (t, 3H, J =6.9 Hz) ppm. ^{13}C NMR (100 MHz, DMSO- d_6): δ =169.3, 139.5, 137.3, 130.2, 129.3, 126.5, 125.9, 41.9, 24.7, 22.5, 14.0, 13.3 ppm. HRMS (ESI-TOF) m/z 224.11063 (224.11091 calcd for $C_{12}H_{18}NOS$, $[M+H^+]$).

4.2.10. *N*-Ethyl-*N*-[2-(propylthio)phenyl]acetamide **3j.** IR ($\nu_{\max}/\text{cm}^{-1}$): 2965, 2932, 2873, 1660 (C=O), 1583, 1470, 1441, 1393, 1298, 1268, 1145, 1063, 1036, 761, 735. ^1H NMR (400 MHz, DMSO- d_6): δ =7.32–7.37 (m, 2H), 7.13–7.21 (m, 2H), 3.87 (dq, 1H, J =13.6,

7.0 Hz), 3.05 (dq, 1H, J =13.1, 6.9 Hz), 2.88 (t, 2H, J =7.3 Hz), 1.59 (s, 3H), 1.50–1.58 (m, 2H), 0.95 (t, 3H, J =7.6 Hz), 0.91 (t, 3H, J =7.6 Hz) ppm. ^{13}C NMR (100 MHz, DMSO- d_6): δ =170.4, 139.2, 137.1, 130.0, 129.5, 126.6, 126.0, 42.2, 32.4, 22.2, 21.9, 13.5, 13.1 ppm. HRMS (ESI-TOF) m/z 238.12530 (238.12656 calcd for $C_{13}H_{20}NOS$, $[M+H^+]$).

4.2.11. *N*-Ethyl-*N*-[2-(hexylthio)phenyl]acetamide **3k.** Previously described.³

4.2.12. *N*-[2-(Benzylthio)phenyl]-*N*-ethylacetamide **3l.** IR ($\nu_{\max}/\text{cm}^{-1}$): 2974, 2922, 2849, 1663 (C=O), 1579, 1494, 1466, 1455, 1379, 1289, 1265, 1063, 1028, 994, 919, 762, 735. ^1H NMR (400 MHz, DMSO- d_6): δ =7.54–7.56 (m, 1H), 7.36–7.42 (m, 3H), 7.29–7.33 (m, 2H), 7.21–7.27 (m, 3H), 4.29 (s, 2H), 3.91 (dq, 1H, J =13.4, 7.2 Hz), 3.04 (dq, 1H, J =14.0, 7.2 Hz), 1.56 (s, 3H), 0.97 (t, 3H, J =7.1 Hz) ppm. ^{13}C NMR (100 MHz, DMSO- d_6): δ =169.2, 139.6, 137.3, 137.1, 130.2, 129.3, 129.3, 129.2, 128.9, 128.9, 127.7, 127.5, 126.4, 45.4, 35.2, 22.4, 13.4 ppm. HRMS (ESI-TOF) m/z 286.12683 (286.12656 calcd for $C_{17}H_{20}NOS$, $[M+H^+]$).

4.2.13. *N*-[2-(Methylthio)phenyl]-*N*-propylacetamide **3m.** IR ($\nu_{\max}/\text{cm}^{-1}$): 2961, 2930, 2872, 1661 (C=O), 1579, 1470, 1374, 1265, 1124, 1068, 1042, 953, 731, 702. ^1H NMR (400 MHz, DMSO- d_6): δ =7.40–7.44 (m, 1H), 7.35 (d, 1H, J =7.8 Hz), 7.23–7.24 (m, 2H), 3.88 (ddd, 1H, J =13.2, 9.2, 6.7 Hz), 2.98 (ddd, 1H, J =13.6, 9.2, 5.9 Hz), 2.47 (s, 3H), 1.64 (s, 3H), 1.34–1.51 (m, 2H), 0.82 (t, 3H, J =7.4 Hz) ppm. ^{13}C NMR (100 MHz, DMSO- d_6): δ =169.5, 139.3, 138.5, 129.9, 129.4, 125.6, 125.5, 48.5, 13.9, 11.7 ppm. HRMS (ESI-TOF) m/z 224.11042 (224.11091 calcd for $C_{12}H_{18}NOS$, $[M+H^+]$).

4.2.14. *N*-[2-(Ethylthio)phenyl]-*N*-propylacetamide **3n.** IR ($\nu_{\max}/\text{cm}^{-1}$): 2965, 2930, 2873, 1656 (C=O), 1583, 1470, 1392, 1295, 1232, 1149, 1096, 1065, 1034, 973, 765, 733. ^1H NMR (400 MHz, DMSO- d_6): δ =7.37–7.42 (m, 2H), 7.20–7.26 (m, 2H), 3.88 (ddd, 1H, J =13.2, 8.8, 7.2 Hz), 3.01 (q, 2H, J =7.4 Hz), 2.97 (ddd, 1H, J =12.7, 9.1, 6.4 Hz), 1.63 (s, 3H), 1.39–1.50 (m, 2H), 1.27 (t, 3H, J =7.3 Hz), 0.82 (t, 3H, J =7.7 Hz) ppm. ^{13}C NMR (100 MHz, DMSO- d_6): δ =170.9, 139.4, 136.7, 130.0, 129.6, 126.6, 126.1, 49.0, 24.7, 22.3, 21.0, 14.0, 11.6 ppm. HRMS (ESI-TOF) m/z 238.12549 (238.12656 calcd for $C_{13}H_{20}NOS$, $[M+H^+]$).

4.2.15. *N*-[2-(Hexylthio)phenyl]-*N*-propylacetamide **3o.** IR ($\nu_{\max}/\text{cm}^{-1}$): 2958, 2928, 2857, 1660 (C=O), 1583, 1469, 1437, 1392, 1295, 1255, 1232, 1149, 1096, 1064, 1036, 733. ^1H NMR (400 MHz, DMSO- d_6): δ =7.36–7.38 (m, 2H), 7.20–7.25 (m, 2H), 3.87 (ddd, 1H, J =13.2, 8.8, 7.8 Hz), 2.99 (t, 2H, J =7.5 Hz), 2.94 (ddd, 1H, J =13.2, 8.8, 6.2 Hz), 1.63 (s, 3H), 1.56–1.62 (m, 2H), 1.37–1.50 (m, 4H), 1.24–1.28 (m, 4H), 0.86 (t, 3H, J =7.0 Hz), 0.82 (t, 3H, J =7.7 Hz) ppm. ^{13}C NMR (100 MHz, DMSO- d_6): δ =169.4, 139.8, 137.3, 130.2, 129.3, 126.6, 125.9, 48.7, 31.2, 30.5, 28.5, 28.4, 22.5, 22.4, 21.2, 14.3, 11.7 ppm. HRMS (ESI-TOF) m/z 294.18792 (294.18916 calcd for $C_{17}H_{28}NOS$, $[M+H^+]$).

4.2.16. *N*-[2-(ethylthio)phenyl]-*N*-hexylacetamide **3p.** IR ($\nu_{\max}/\text{cm}^{-1}$): 2955, 2927, 2857, 1660 (C=O), 1583, 1528, 1469, 1456, 1392, 1374, 1309, 1241, 1171, 1156, 1126, 1096, 1065, 1034, 1015, 758, 733. ^1H NMR (400 MHz, DMSO- d_6): δ =7.37–7.42 (m, 2H), 7.21–7.26 (m, 2H), 3.91 (ddd, 1H, J =13.6, 9.6, 6.5 Hz), 3.01 (q, 2H, J =7.5 Hz), 2.94–3.02 (m, 1H, under q at 3.01 ppm), 1.63 (s, 3H), 1.36–1.47 (m, 2H), 1.27 (t, 3H, J =7.2 Hz), 1.17–1.25 (m, 6H), 0.83 (t, 3H, J =6.8 Hz) ppm. ^{13}C NMR (100 MHz, DMSO- d_6): δ =170.8, 139.4, 136.8, 129.9, 129.5, 126.6, 126.1, 47.3, 31.3, 27.6, 26.3, 24.7, 22.3, 22.3, 14.2, 14.0 ppm. HRMS (ESI-TOF) m/z 280.17253 (280.17351 calcd for $C_{16}H_{26}NOS$, $[M+H^+]$).

4.2.17. *N*-Hexyl-*N*-[2-(propylthio)phenyl]acetamide **3q.** IR ($\nu_{\max}/\text{cm}^{-1}$): 2959, 2927, 2857, 1660 (C=O), 1583, 1528, 1470, 1456, 1434,

1393, 1300, 1260, 1241, 1171, 1157, 1126, 1095, 1065, 1015, 795, 745, 729. ¹H NMR (400 MHz, DMSO-*d*₆): δ=7.35–7.42 (m, 2H), 7.18–7.26 (m, 2H), 3.90 (ddd, 1H, *J*=13.2, 9.2, 6.7 Hz), 3.02 (ddt, 1H, *J*=13.3, 9.06, 5.0 Hz), 2.98 (t, 2H, *J*=7.1 Hz), 1.64 (s, 3H), 1.58–1.67 (m, 2H), 1.36–1.47 (m, 2H), 1.19–1.26 (m, 6H), 0.99 (t, 3H, *J*=7.1 Hz), 0.83 (t, 3H, *J*=6.8 Hz) ppm. ¹³C NMR (100 MHz, DMSO-*d*₆): δ=169.4, 139.9, 137.3, 130.3, 129.3, 126.6, 125.9, 47.0, 32.4, 31.5, 27.8, 26.6, 22.5, 22.4, 22.0, 14.4, 13.7 ppm. HRMS (ESI-TOF) *m/z* 294.18892 (294.18916 calcd for C₁₇H₂₈NOS, [M+H⁺]).

4.2.18. *N*-Benzyl-*N*-[2-(ethylthio)phenyl]acetamide **3r**. IR ($\nu_{\max}/\text{cm}^{-1}$): 2969, 2926, 2869, 1653 (C=O), 1582, 1467, 1434, 1388, 1280, 1249, 1209, 1064, 1030, 970, 774, 759, 700. ¹H NMR (400 MHz, DMSO-*d*₆): δ=7.41 (dd, 1H, *J*=8.0, 1.4 Hz), 7.34 (dt, 1H, *J*=7.6, 1.6 Hz), 7.22–7.30 (m, 3H), 7.17–7.20 (m, 2H), 7.06 (dt, 1H, *J*=7.5, 1.6 Hz), 6.80 (dd, 1H, *J*=7.9, 1.4 Hz), 5.42 (d, 1H, *J*=14.2 Hz), 3.97 (d, 1H, *J*=14.2 Hz), 3.02 (dq, 2H, *J*=7.3, 3.0 Hz), 1.72 (s, 3H), 1.28 (t, 3H, *J*=7.2 Hz) ppm. ¹³C NMR (100 MHz, DMSO-*d*₆): δ=170.0, 139.4, 137.9, 137.0, 130.2, 129.4, 128.9, 128.9, 128.7, 128.7, 127.7, 126.7, 125.7, 50.3, 24.7, 22.4, 14.1 ppm. HRMS (ESI-TOF) *m/z* 286.12667 (286.12656 calcd for C₁₇H₂₀NOS, [M+H⁺]).

4.2.19. *N*-Benzyl-*N*-[2-(benzylthio)phenyl]acetamide **3s**. IR ($\nu_{\max}/\text{cm}^{-1}$): 3028, 2926, 1655 (C=O), 1582, 1494, 1469, 1454, 1435, 1386, 1357, 1284, 1210, 1064, 1029, 971, 776, 755, 729, 698. ¹H NMR (400 MHz, DMSO-*d*₆): δ=7.56 (dd, 1H, *J*=8.1, 1.6 Hz), 7.40–7.43 (m, 2H), 7.29–7.35 (m, 3H), 7.20–7.28 (m, 4H), 7.10–7.13 (m, 2H), 7.06 (dt, 1H, *J*=7.5, 1.2 Hz), 6.77 (dd, 1H, *J*=7.7, 1.2 Hz), 5.37 (d, 1H, *J*=14.7 Hz), 4.30 (s, 2H), 3.86 (d, 1H, *J*=13.9 Hz), 1.64 (s, 3H) ppm. ¹³C NMR (100 MHz, DMSO-*d*₆): δ=170.0, 139.7, 137.8, 137.7, 136.7, 130.2, 129.4, 129.3, 129.0, 128.9, 128.7, 128.0, 127.7, 127.6, 126.2, 50.5, 35.4, 22.4 ppm. HRMS (ESI-TOF) *m/z* 348.14149 (348.14221 calcd for C₂₂H₂₂NOS, [M+H⁺]).

4.2.20. *N*-[2-(Ethylthio)phenyl]-*N*-(2-methylbenzyl)acetamide **3t**. IR ($\nu_{\max}/\text{cm}^{-1}$): 2970, 2929, 2872, 1658 (C=O), 1584, 1471, 1440, 1386, 1379, 1359, 1301, 1271, 1248, 1049, 1040, 969, 764, 738. ¹H NMR (400 MHz, DMSO-*d*₆): δ=7.40 (dd, 1H, *J*=8.0, 1.3 Hz), 7.32 (dt, 1H, *J*=7.6, 1.4 Hz), 7.09–7.14 (m, 2H), 7.04–7.08 (m, 2H), 7.02 (dd, 1H, *J*=7.5, 1.4 Hz), 6.74 (dd, 1H, *J*=7.8, 1.3 Hz), 5.34 (d, 1H, *J*=14.7 Hz), 4.18 (d, 1H, *J*=14.7 Hz), 3.02 (q, 2H, *J*=7.3 Hz), 2.06 (s, 3H), 1.71 (s, 3H), 1.27 (t, 3H, *J*=7.3 Hz) ppm. ¹³C NMR (100 MHz, DMSO-*d*₆): δ=169.7, 139.1, 137.0, 136.8, 135.5, 130.4, 130.2, 129.8, 129.4, 127.8, 126.7, 126.2, 125.7, 47.2, 24.8, 22.4, 19.0, 14.2 ppm. HRMS (ESI-TOF) *m/z* 300.14192 (300.14221 calcd for C₁₈H₂₂NOS, [M+H⁺]).

4.2.21. *N*-(2-Methylphenyl)-*N*-[2-(2-methylbenzylthio)phenyl]acetamide **3u**. IR ($\nu_{\max}/\text{cm}^{-1}$): 3051, 3021, 2979, 2927, 1655 (C=O), 1584, 1493, 1471, 1391, 1265, 1050, 1037, 971, 730, 702. ¹H NMR (400 MHz, DMSO-*d*₆): δ=7.59 (dd, 1H, *J*=8.0, 1.0 Hz), 7.34 (dt, 1H, *J*=7.7, 1.4 Hz), 7.28 (d, 1H, *J*=7.5 Hz), 7.17–7.22 (m, 2H), 7.01–7.14 (m, 5H), 6.94 (d, 1H, *J*=7.3 Hz), 6.73 (dd, 1H, *J*=7.8, 1.2 Hz), 5.30 (d, 1H, *J*=14.7 Hz), 4.24–4.30 (m, 2H), 4.05 (d, 1H, *J*=14.7 Hz), 2.40 (s, 3H), 2.03 (s, 3H), 1.64 (s, 3H) ppm. ¹³C NMR (100 MHz, DMSO-*d*₆): δ=169.6, 139.5, 137.2, 136.7, 135.4, 134.7, 130.9, 130.4, 130.2, 130.1, 129.8, 129.3, 128.3, 128.1, 127.8, 126.4, 126.3, 126.1, 55.4, 49.1, 34.2, 22.3, 19.0 ppm. HRMS (ESI-TOF) *m/z* 376.17314 (376.17351 calcd for C₂₄H₂₆NOS, [M+H⁺]).

4.2.22. *N*-Ethyl-*N*-[2-(ethylseleno)phenyl]acetamide **3v**. IR ($\nu_{\max}/\text{cm}^{-1}$): 2972, 2930, 2872, 1655 (C=O), 1582, 1470, 1441, 1392, 1376, 1297, 1263, 1144, 1161, 1102, 1063, 1035, 994, 760, 734. ¹H NMR (400 MHz, DMSO-*d*₆): δ=7.50 (dd, 1H, *J*=7.9, 1.2 Hz), 7.37 (dt, 1H, *J*=7.3, 1.8 Hz), 7.30 (dt, 1H, *J*=7.9, 1.2 Hz), 7.25 (dd, 1H, *J*=7.6, 1.8 Hz), 3.94 (dq, 1H, *J*=14.0, 7.0 Hz), 3.08 (dq, 1H, *J*=14.0, 7.0 Hz), 3.00 (q, 2H, *J*=7.5 Hz), 1.64 (s, 3H), 1.40 (t, 3H, *J*=7.8 Hz), 1.02 (t, 3H,

J=7.8 Hz) ppm. ¹³C NMR (100 MHz, DMSO-*d*₆): δ=169.2, 141.4, 133.0, 130.4, 129.7, 129.5, 127.1, 42.1, 22.8, 18.7, 15.2, 13.5 ppm. HRMS (ESI-TOF) *m/z* 272.05426 (272.05536 calcd for C₁₂H₁₈NOSe, [M+H⁺]).

4.2.23. *N*-Ethyl-*N*-[2-(hexylseleno)phenyl]acetamide **3w**. IR ($\nu_{\max}/\text{cm}^{-1}$): 2957, 2928, 2855, 1656 (C=O), 1579, 1467, 1441, 1390, 1375, 1296, 1265, 1144, 1099, 1051, 1030, 993, 917, 759, 729. ¹H NMR (400 MHz, DMSO-*d*₆): δ=7.50 (dd, 1H, *J*=7.8, 1.3 Hz), 7.36 (dt, 1H, *J*=7.5, 1.6 Hz), 7.29 (dt, 1H, *J*=7.2, 1.4 Hz), 7.24 (dd, 1H, *J*=7.6, 1.6 Hz), 3.95 (dq, 1H, *J*=13.7, 7.0 Hz), 3.08 (dq, 1H, *J*=13.7, 7.0 Hz), 3.00 (t, 2H, *J*=7.5 Hz), 1.65–1.70 (m, 2H), 1.64 (s, 3H), 1.29–1.41 (m, 2H), 1.24–1.28 (m, 4H), 1.02 (t, 3H, *J*=7.2 Hz), 0.85 (t, 3H, *J*=6.8 Hz) ppm. ¹³C NMR (100 MHz, DMSO-*d*₆): δ=169.1, 141.3, 133.2, 130.3, 129.7, 129.5, 127.0, 42.1, 31.1, 29.5, 29.4, 25.1, 22.7, 22.4, 14.3, 13.4 ppm. HRMS (ESI-TOF) *m/z* 328.11670 (328.11796 calcd for C₁₆H₂₆NOSe, [M+H⁺]).

4.2.24. *N,N*-Diethyl-2-(ethylthio)aniline **4a**. IR ($\nu_{\max}/\text{cm}^{-1}$): 2977, 2929, 1584, 1471, 1391, 1303, 1265, 1067, 1050, 730, 702. ¹H NMR (400 MHz, DMSO-*d*₆): δ=7.15–7.18 (m, 1H), 7.04–7.12 (m, 3H), 2.96 (q, 4H, *J*=7.1 Hz), 2.85 (q, 2H, *J*=7.3 Hz), 1.26 (t, 3H, *J*=7.3 Hz), 0.92 (t, 6H, *J*=7.1 Hz) ppm. ¹³C NMR (100 MHz, DMSO-*d*₆): δ=147.8, 136.5, 125.7, 124.9, 123.1, 47.1, 24.4, 14.1, 12.7 ppm. HRMS (ESI-TOF) *m/z* 210.13053 (210.13165 calcd for C₁₂H₂₀NS, [M+H⁺]).

4.2.25. *N*-Ethyl-2-(methylthio)-*N*-propylaniline **4b**. IR ($\nu_{\max}/\text{cm}^{-1}$): 2959, 2920, 2871, 2810, 1578, 1470, 1438, 1379, 1268, 1225, 1171, 1126, 1084, 1068, 1042, 752, 731. ¹H NMR (400 MHz, DMSO-*d*₆): δ=7.10–7.12 (m, 2H), 7.07–7.09 (m, 2H), 2.93 (q, 2H, *J*=7.1 Hz), 2.87 (t, 2H, *J*=7.2 Hz), 2.31 (s, 3H), 1.34 (sext, 2H, *J*=7.3 Hz), 0.93 (t, 3H, *J*=7.1 Hz), 0.82 (t, 3H, *J*=7.4 Hz) ppm. ¹³C NMR (100 MHz, DMSO-*d*₆): δ=147.7, 138.0, 125.1, 124.5, 124.2, 123.0, 54.5, 48.0, 20.6, 13.9, 12.5, 12.1 ppm. HRMS (ESI-TOF) *m/z* 210.13139 (210.13165 calcd for C₁₂H₂₀NS, [M+H⁺]).

4.3. VT-NMR spectroscopy

VT-NMR experiments were run on a Bruker Avance 400 MHz spectrometer equipped with a variable temperature probe. Temperature calibrations were performed before the experiments by means of a thermocouple with an uncertainty not exceeding ±2 K. The conditions were kept as equal as possible with all subsequent work. To selectively irradiate the desired signal, a 50 Hz wide shaped pulse was calculated with a refocusing-SNOB shape¹⁰ and a pulse width of 37 ms.

4.4. In vitro cell viability studies using MCF-7, NHDF, and LNCaP cells

The cells used in this study were human breast (MCF-7) and prostate (LNCaP) cancer cells as well as normal human dermal fibroblasts (NHDF) (all acquired to ATCC—American Type Culture Collection).

Unless otherwise stated, chemicals (analytical grade), assay reagents, culture media, and supplements are all from Sigma–Aldrich.

The studied compounds were dissolved in dimethylsulfoxide (DMSO) and the final solvent concentration in the MTT experiment was 0.3%. This concentration of DMSO has no significant effect on cell viability (data not shown).

4.4.1. *Culture of cells*. Cells were routinely maintained in 75 or 150 cm² T-flasks at 37 °C in a humidified atmosphere containing 5% CO₂. Human dermal fibroblasts were cultured in RPMI medium supplemented with 10% fetal bovine serum (FBS), HEPES (0.01 M), L-glutamine (0.02 M), and sodium pyruvate (0.001 M) and 1% antibiotic/antimycotic (10,000 units/ml penicillin, 10 mg/ml

streptomycin and 25 µg/ml amphotericin B). Dubelco's Modified Eagle's Medium high glucose supplemented with 10% fetal bovine serum and 1% antibiotic/antimycotic was used to culture MCF-7 cells. LNCaP cells were cultured in RPMI medium supplemented with 10% FBS and 1% antibiotic (10,000 units/ml penicillin and 10 mg/ml streptomycin). The cells used in the experiments were in passages 5–6 (NHDF), 36–37 (MCF-7), and 23–24 (LNCaP).

4.4.2. MTT assay. Cell viability was evaluated by quantifying the extent of the reduction of 3-(4,5-dimethylthiazol-2-yl)-2,5-diphenyltetrazolium bromide (MTT) according to a previously described procedure.⁹ Briefly, cells were seeded in 48-well plates (0.5×10^4 cells/well) in the culture medium and after 48 h they were treated with the different compounds at 30 µM for 48 h, with untreated cells serving as negative control and H₂O₂ (1 mM) as positive control. For the dose–response studies, the concentrations evaluated were 0.01, 0.1, 1, 10, 50, and 100 µM. At the end of incubation the media in wells were removed and replaced with fresh media and MTT solution (5 mg/ml in phosphate buffer saline) and incubated at 37 °C for 4 h. Thereafter, media-containing MTT were removed and formazan crystals were dissolved with DMSO and absorbance was recorded in an Anthus 2020 microplate reader at 570 nm. The extent of cell death was expressed as the percentage of cell viability in comparison with control cells.

4.4.3. Statistics. The experiments were performed in quintuplicate and the results of the cell proliferation were expressed as average ± standard deviation (SD). These calculations as well as the quantification of the potential association between the lipophilicity (log *P*) and cytotoxic effects were performed using the program Microsoft Excel 2010. The half-medium inhibitory concentration (IC₅₀) values were calculated from the obtained dose–response curve by sigmoid fitting.

Acknowledgements

This work was financed by FCT (Project PTDC/QUI-QUI/100896/2008) and COMPETE (Project Pest-C/SAU/UI0709/2011).

References and notes

- Curran, D. P.; Qi, H.; Geib, S. J.; DeMello, N. C. *J. Am. Chem. Soc.* **1994**, *116*, 3131.
- (a) Brandes, S.; Niess, B.; Bella, M.; Prieto, A.; Overgaard, J.; Jørgensen, K. A. *Chem.—Eur. J.* **2006**, *12*, 6039; (b) Brandes, S.; Bella, M.; Kjærsgaard, A.; Jørgensen, K. A. *Angew. Chem., Int. Ed.* **2006**, *45*, 1147; (c) Ishichi, Y.; Ikeura, Y.; Natsugari, H. *Tetrahedron* **2004**, *60*, 4481; (d) Albert, J. S.; Ohnmacht, C.; Bernstein, P. R.; Rumsey, W. L.; Aharony, D.; Masek, B. B.; Dembofsky, B. T.; Koether, G. M.; Potts, W.; Evenden, J. L. *Tetrahedron* **2004**, *60*, 4337; (e) Curran, D. P.; Chen, C. H.-T.; Geib, S. J.; Lapiere, A. J. B. *Tetrahedron* **2004**, *60*, 4413; (f) Clayden, J.; McCarthy, C.; Helliwell, M. *Chem. Commun.* **1999**, 2059; (g) Curran, D. P.; Geib, S. J.; DeMello, N. C. *Tetrahedron* **1999**, *55*, 5681; (h) Curran, D. P.; Liu, W.; Chen, C. H.-T. *J. Am. Chem. Soc.* **1999**, *121*, 11012; (i) Avalos, M.; Babiano, R.; Cintas, P.; Higes, F. J.; Jiménez, J. L.; Palacios, J. C.; Silvero, G. *Tetrahedron: Asymmetry* **1999**, *10*, 4071; (j) Fujita, M.; Kitagawa, O.; Izawa, H.; Dobashi, A.; Fukaya, H.; Taguchi, T. *Tetrahedron Lett.* **1999**, *40*, 1949; (k) Clayden, J. *Synlett* **1998**, 810; (l) Ikeura, Y.; Ishichi, Y.; Tanaka, T.; Fujishima, A.; Murabayashi, M.; Kawada, M.; Ishimaru, T.; Kamo, I.; Doi, T.; Natsugari, H. *J. Med. Chem.* **1998**, *41*, 4232; (m) Ikeura, Y.; Ishimaru, T.; Doi, T.; Kawada, M.; Fujishima, A.; Natsugari, H. *Chem. Commun.* **1998**, 2141; (n) Kitagawa, O.; Izawa, H.; Sato, K.; Dobashi, A.; Taguchi, T. *J. Org. Chem.* **1998**, *63*, 2634; (o) Ahmed, A.; Bragg, R. A.; Clayden, J.; Lai, L. W.; McCarthy, C.; Pink, J. H.; Westlund, N.; Yasin, S. A. *Tetrahedron* **1998**, *54*, 13277; (p) Clayden, J. *Angew. Chem., Int. Ed.* **1997**, *36*, 949; (q) Curran, D. P.; Hale, G. R.; Geib, S. J.; Balog, A.; Cass, Q. B.; Degani, A. L. G.; Hernandez, M. Z.; Freitas, L. C. G. *Tetrahedron: Asymmetry* **1997**, *8*, 3955; (r) Clayden, J.; Westlund, N.; Wilson, F. X. *Tetrahedron Lett.* **1996**, *37*, 5577; (s) Thayumanavan, S.; Beak, P.; Curran, D. P. *Tetrahedron Lett.* **1996**, *37*, 2899; (t) Hughes, A. D.; Price, D. A.; Shishkin, O.; Simpkins, N. S. *Tetrahedron Lett.* **1996**, *37*, 7607; (u) Bowles, P. J.; Clayden, J. M.; Tomkinson, M. *Tetrahedron Lett.* **1995**, *36*, 9219.
- Ramos, S. S.; Reis, L. V.; Boto, R. E. F.; Santos, P. F.; Almeida, P. *Tetrahedron Lett.* **2013**, *54*, 5441.
- Representative examples: (a) Siddall, T. H., III. *J. Org. Chem.* **1966**, *31*, 3719; (b) Siddall, T. H., III; Steward, W. E. *J. Org. Chem.* **1969**, *34*, 2927; (c) Steward, W. E.; Siddall, T. H., III. *Chem. Rev.* **1970**, *70*, 517; (d) Staskun, B. *J. Org. Chem.* **1981**, *46*, 1643.
- Yamasaki, R.; Tanatani, A.; Azumaya, I.; Saito, S.; Yamaguchi, K.; Kagechika, H. *Org. Lett.* **2003**, *5*, 1265.
- Eyring, H. *Chem. Rev.* **1935**, *17*, 65.
- Representative examples: (a) Shvo, Y.; Taylor, E. C.; Mislow, K.; Raban, M. *J. Am. Chem. Soc.* **1967**, *89*, 4910; (b) Siddall, T. H., III; Steward, W. E. *J. Phys. Chem.* **1969**, *73*, 40; (c) Kondo, O. K.; Iida, T.; Fujita, H.; Suzuki, T.; Yamaguchi, K.; Murakami, Y. *Tetrahedron* **2000**, *56*, 8883; (d) Ates, A.; Curran, D. P. *J. Am. Chem. Soc.* **2001**, *123*, 5130; (e) Clayden, J., Ed. (Tetrahedron Symposium in-Print on Axially Chiral Amides) *Tetrahedron* **2004**, *60*, 4325–4558; (f) Kitagawa, O.; Yoshikawa, M.; Tanabe, H.; Morita, T.; Takahashi, M.; Dobashi, Y.; Taguchi, T. *J. Am. Chem. Soc.* **2006**, *128*, 12923.
- (a) Kankanala, K.; Reddy, V. R.; Devi, Y. P.; Mangamoori, L. N.; Mukkanti, K.; Pal, S. *J. Chem.* **2013**, *1*–8 <http://dx.doi.org/10.1155/2013/816769> Hindawi Publishing Corporation, <http://www.hindawi.com/journals/jchem/>; (b) Mareddy, J.; Nallapati, S. B.; Anireddy, J.; Devi, Y. P.; Mangamoori, L. N.; Kapavarapu, R.; Pal, S. *Bioorg. Med. Chem. Lett.* **2013**, *23*, 6721; (c) Zhong, B.; Cai, X. H.; Chennamaneni, S.; Yi, X.; Liu, L. L.; Pink, J. J.; Dowlati, A.; Xu, Y.; Zhou, A. M.; Su, B. *Eur. J. Med. Chem.* **2012**, *47*, 432; (d) Zhong, B.; Lama, R.; Smith, K. M.; Xu, Y.; Su, B. *Bioorg. Med. Chem. Lett.* **2011**, *21*, 5324; (e) Su, B.; Chen, S. A. *Bioorg. Med. Chem. Lett.* **2009**, *19*, 6733; (f) Su, B.; Darby, M. V.; Brueggemeier, R. W. *J. Med. Chem.* **2008**, *10*, 475; (g) Su, B.; Diaz-Cruz, E. S.; Landini, S.; Brueggemeier, R. W. *J. Med. Chem.* **2006**, *49*, 1413; (h) Su, B.; Landini, S.; Davis, D. D.; Brueggemeier, R. W. *J. Med. Chem.* **2007**, *50*, 1635; (i) Su, B.; Tian, R.; Darby, M. V.; Brueggemeier, R. W. *J. Med. Chem.* **2008**, *51*, 1126.
- (a) Cruz, C.; Cairrão, E.; Silvestre, S.; Breitenfeld, L.; Almeida, P.; Queiroz, J. A. *PLoS One* **2011**, *6*, e27078; (b) Cytotoxicity In Culture of Animal Cells: A Manual of Basic Technique; Freshney, R. I., Ed.; John Wiley & Sons: Hoboken, NJ, 2005; Chapter 22, pp 359–373.
- Kupče, E.; Boyd, J.; Campbell, I. D. *J. Magn. Reson., Ser. B* **1995**, *106*, 300.